Stratification of glioma based on stemness scores in bulk and single-cell transcriptomes

Abdelrahman, Z., Abdelatty, A., Luo, J., McKnight, A. J., & Wang, X. (2024). Stratification of glioma based on stemness scores in bulk and single-cell transcriptomes. *Computers in Biology and Medicine*, *175*, Article 108304. https://doi.org/10.1016/j.compbiomed.2024.108304

Published in:
Computers in Biology and Medicine

Document Version:
Publisher's PDF, also known as Version of record

Computers in Biology and Medicine 175 (2024) 108304

Contents lists available at ScienceDirect

Computers in Biology and Medicine

journal homepage: www.elsevier.com/locate/compbiomed

Stratification of glioma based on stemness scores in bulk and single-cell transcriptomes

Zeinab Abdelrahman [a,*,1], Alaa Abdelatty [b,1], Jiangti Luo [c,d,e], Amy Jayne McKnight [a], Xiaosheng Wang [c,d,e,**]

[a] Molecular Epidemiology and Public Health Research Group, Centre for Public Health, Queen's University Belfast, Institute for Clinical Sciences A, Royal Victoria Hospital, Belfast, BT12 6BA, UK
[b] Department of Pathology, Faculty of Veterinary Medicine, Kafrelsheikh University, Kafrelsheikh, Egypt
[c] Biomedical Informatics Research Lab, School of Basic Medicine and Clinical Pharmacy, China Pharmaceutical University, Nanjing, 211198, China
[d] Cancer Genomics Research Center, School of Basic Medicine and Clinical Pharmacy, China Pharmaceutical University, Nanjing, 211198, China
[e] Big Data Research Institute, China Pharmaceutical University, Nanjing, 211198, China

ARTICLE INFO

Keywords:
Glioma
Stemness
Clustering analysis
Stemness subtypes
Molecular features

ABSTRACT

Background: Brain tumours are known to have a high mortality and morbidity rate due to their localised and frequent invasive growth. The concept that glioma resistance could originate from the dissimilarity in the vulnerability of clonogenic glial stem cells to chemotherapeutic drugs and radiation has driven the scientific community to reexamine the comprehension of glioma growth and strategies that target these cells or modify their stemness.

Methods: Based on the enrichment scores of 12 stemness signatures, we identified glioma subtypes in both tumour bulks and single cells by clustering analysis. Furthermore, we comprehensively compared molecular and clinical features among the glioma subtypes.

Results: Consistently, in seven different datasets, hierarchical clustering uncovered three subtypes of glioma, termed Stem-H, Stem-M, and Stem-L, with high, medium, and low stemness signatures, respectively. Stem-H and Stem-L exhibited the most unfavorable and favourable overall and disease-free survival, respectively. Stem-H showed the highest enrichment scores of the EMT, invasion, proliferation, differentiation, and metastasis processes signatures, while Stem-L displayed the lowest. Stem-H harboured a greater proportion of late-stage tumours compared to Stem-L. Moreover, Stem-H manifested higher tumour mutation burden, DNA damage repair and cell cycle activity, intratumour heterogeneity, and a more frequent incidence of *TP53* and *EGFR* mutations than Stem-L. In contrast, Stem-L had higher O6-Methylguanine-DNA Methyltransferase (**MGMT**) methylation levels.

Conclusion: The classification of glioma based on stemness may offer new insights into the biology of the tumour, as well as more accurate clinical management of the disease.

1. Introduction

Brain tumours are known to have a high mortality and morbidity rate due to their localised and frequent invasive growth [1]. Gliomas represent approximately 30% of all primary brain tumours and 80% of all malignant ones [2]. Brain tumours are divided histologically into astrocytomas, oligodendrogliomas, hybrid oligoastrocytic gliomas, and ependymomas according to resemblances in shape to the neuroglial cells found in a healthy brain [1]. Categorisation has progressed further based on the tumour position, distinguishing patterns, and features of anaplasia. The glioma malignancy grades (I to IV) from the World Health Organization (WHO) are determined by the presence or absence of anaplastic features [1]. Beyond histological classification, molecular classification may furnish diagnostic, prognostic, and treatment values

* Corresponding author.
** Corresponding author. Biomedical Informatics Research Lab, School of Basic Medicine and Clinical Pharmacy, China Pharmaceutical University, Nanjing, 211198, China.
E-mail addresses: z.abdelrahman@qub.ac.uk (Z. Abdelrahman), xiaosheng.wang@cpu.edu.cn (X. Wang).
[1] Equal contribution.

https://doi.org/10.1016/j.compbiomed.2024.108304
Received 28 October 2023; Received in revised form 7 March 2024; Accepted 12 March 2024
Available online 22 March 2024

for glioma [3]. In addition, the tumour microenvironment (TME) is essential in influencing cancer progression, metastasis, and the response to treatment [4]. Glioma cells can produce a variety of chemokines, cytokines, and growth factors that promote the infiltration of diverse cells and immune cells in the TME [5].

Glioblastoma (GBM) is a glioma characterised by rapid growth and difficulty in surgical removal [5]. Based on gene expression profiles, GBMs can be divided into four subtypes, including classical, proneural, neural, and mesenchymal, with different levels of aggressiveness and progression and distinct prognoses [6]. Malignant cells may exhibit stem-like features [7] to maintain cancer progression [8]. Drug resistance of GBM could originate from the dissimilarity in the vulnerability of clonogenic glial stem cells to chemotherapeutic drugs, and radiation may target these cells or modify their stemness [9].

Gaining a comprehensive understanding of the complexities of cancer stemness in glioma is of utmost importance in deciphering the molecular and clinical intricacies of this debilitating brain tumor. Our objective was to gain insights into the inherent heterogeneity of gliomas and its correlation with key molecular and clinical characteristics through a thorough classification of gliomas based on stemness signatures using transcriptomic data. By conducting data analysis on seven glioma datasets, we have discovered the presence of three distinct stemness subtypes within the tumor landscape. These subtypes, which are categorized as high, medium, and low stemness clusters, were detected in both bulk tumor samples and at the single-cell level. This classification not only enhances our understanding of glioma heterogeneity but also provides vital insights into the molecular mechanisms underlying cancer stem cells.

By addressing the limitations of previous research on molecular subtypes and stemness characteristics of glioma, this study makes a substantial contribution to the field. Previous investigations [10,11], primarily based on bulk RNA-seq data, have provided valuable insights; however, they may not comprehensively capture the complex nature of intra-tumoral heterogeneity (ITH) observed in glioma. The distinctive feature of our research lies in the utilization of single-cell RNA-seq data analysis, facilitating a more intricate investigation of the tumor microenvironment, specifically the recognition and classification of rare cell populations such as Glioma Stem Cells (GSCs).

2. Methods

2.1. Datasets

We downloaded five gene expression profiling datasets for gliomas, including TCGA-glioma (GBM and low-grade glioma (LGG)) from the Genomic Data Commons (GDC) (https://portal.gdc.cancer.gov/), GSE16011 [12] and GSE109857 [13] from the NCBI gene expression omnibus (https://www.ncbi.nlm.nih.gov/geo/), and CGGA301 and CGGA325 from the Chinese Glioma Genome Atlas (http://www.cgga.org.cn/). Additionally, we acquired the somatic copy number alterations (sCNAs) data (referred to as "SNP6" files) of TCGA-glioma and TCGA protein expression data from GDC. Besides, we downloaded glioma single-cell RNA sequencing (scRNA-seq) datasets, including GSE131928 [14], GSE89567 [15], and GSE57872 [16], from the NCBI gene expression omnibus. A description of these datasets is shown in the Supplementary Table.

2.2. Aggregation of stemness signatures

We retrieved 12 signatures of stem cells or stemness from the StemChecker webserver (http://stemchecker.sysbiolab.eu) for Homo sapiens [17]. The stemness signatures were obtained through various techniques, such as gene expression profiles, literature curation, computational methods, transcription factor target genes, and RNAi screening [17]. The 12 stemness signatures and their corresponding marker genes are presented in the Supplementary Table. Through the application of hierarchical clustering, we systematically arranged and categorized the 36 human stemness signatures, unveiling patterns of similarity and dissimilarity within the group. Through this process, we identified clusters with comparable stemness features. As a result, we have identified the top 12 signatures that demonstrated the most cohesive and distinct patterns through the hierarchical clustering analysis (Compilation of datasets from the StemChecker web server utilized in the present study presented in the Supplementary Table).

2.3. Analysis of gene-set enrichment

Utilizing the single-sample gene-set enrichment analysis (ssGSEA) [18], we assessed the enrichment score of a gene set that represents a stemness signature, biological process, or pathways, in a tumour bulk or single cell. The ssGSEA computes the enrichment score of a gene set in a sample based on its expression profiles. The ssGSEA was executed using the 'GSVA' R package. The gene sets were acquired from their corresponding publications or related databases, shown in the Supplementary Table.

2.4. Clustering analysis

The glioma subtypes were identified through hierarchical clustering, utilizing the normalized enrichment scores (scale normalization) derived from the 12 stemness gene sets. Clustering analysis was conducted using the 'pheatmap' R package [19]. The distance metric for column clustering was set to 'Euclidean,' and the clustering method was 'complete.'

2.5. Survival analysis

The survival time was compared using Kaplan-Meier curves [20], and the significance of survival time differences was evaluated using log-rank tests. Survival analyses were performed using the "survfit" function available in the "survival" R package [21].

2.6. Pathway and gene ontology analysis (WGCNA)

We identified the KEGG and GO pathways highly enriched in Stem-H and Stem-L gliomas by ClusterProfiler R package [22] with a threshold of adjusted P value < 0.05. We identified the gene modules (gene ontology) highly enriched in Stem-H and Stem-L gliomas using WGCNA [23].

2.7. The assessment of tumour mutation burden (TMB), somatic copy number alterations (SCNA), intratumour heterogeneity (ITH), immune score, stromal score, and tumour purity

TMB is defined as the total number of somatic mutations in the tumour. Arm- and focal-level SCNAs, as well as G-scores in tumours were calculated using GISTIC2 [24], with the input of 'SNP6' files. The G-score represents the amplitude and frequency of CNA occurrences observed across a group of samples. The DITHER algorithm [25] assessed ITH levels by scoring ITH according to the entropies of somatic mutation profiles and SCNA profiles within the tumour. We used ESTIMATE [26] to determine each tumour sample's immune score, stromal score, and tumour purity. The immune score, stromal score, and tumour purity parameters illustrate the extent of immune infiltration, stromal content, and proportion of tumour cells in the tumour bulk.

2.8. Evaluation of proportions of immune cell subsets in tumours

The CIBERSORT algorithm [27] was used to evaluate the proportions of 22 human immune cell subsets. CIBERSORT is an analytical tool for estimating the abundance of member cell types present in a mixed cell population [28]. The execution of the CIBERSORT algorithm involved

1000 permutations, and the sample deconvolution success was evaluated based on a threshold of *P*-value less than 0.05.

2.9. Logistic regression analysis

We applied logistic regression using two predictors, stemness cluster and tumour purity, to predict the stemness score and EMT signature score (high > median score and low < median score). The predictors were expressed as binary variables. Tumour purity was designated as either 1 (high > median score) or 0 (low < median score), while stemness cluster was classified as either 1 (belonging to Stem-H and Stem-M) or 0 (Stem-L). We employed the R function "glm" to fit the binary model during the logistic regression analyses.

2.10. Pseudotime analysis

To deduce the phylogenetic correlation between high- and low-stemness tumour bulks or cells, we constructed their trajectory path using Monocle3 [29]. The capabilities of Monocle3 encompass cell clustering, classification, and counting, along with trajectory construction and differential expression analysis within those trajectories.

2.11. Anti-tumour compounds sensitivity analysis

We used the TIDE algorithm [30] to predict the response to immunotherapy. An increase in the TIDE prediction score indicates a greater probability of immune escape and a reduced probability of a positive response to immunotherapy for the patient.

2.12. scRNA-seq data analysis

We analyzed a SMART-seq2 dataset comprising gene expression profiles of 543, 7930, and 6341 cancer cells from the scRNA-seq datasets GSE57872, GSE131928, and GSE89567, respectively. SingleR, a computational method that uses transcriptomic datasets of individual cell types as reference [31], was used to identify cell types based on scRNA-seq data. The clustering of individual cells was accomplished by using the t-distributed stochastic neighbor embedding (t-SNE) algorithm [32], which produces a solitary map that exhibits structure at multiple levels.

2.13. Statistical analysis

The comparison between two classes of normally distributed data, including gene and protein expression levels, was performed using Student's *t*-tests (two-tailed). To compare two classes of non-normally distributed data, we employed the Mann-Whitney *U* test (one-tailed). In the comparison of three classes of data, the ANOVA (for normally distributed data) or Kruskal-Wallis (K–W) tests (non-normally distributed data) were employed. To determine the associations between two categorical variables, we employed the Fisher's exact test or Chi-square test. The false discovery rate (FDR) was evaluated using the Benjamini-Hochberg method [33] for multiple test adjustments.

3. Results

3.1. Identification of stemness subtypes of glioma in tumour bulks

Based on the ssGSEA scores of 12 stemness signatures, hierarchical clustering identified three clusters of glioma, consistent in five datasets, namely TCGA-glioma cohort, CGGA301, CGGA325, GSE16011, and GSE109857. The three clusters were termed Stem-H, Stem-M, and Stem-L, characterized by high, medium, and low scores of stemness signatures, respectively (Fig. 1A). By comparing the enrichment scores of a 109-gene stemness signature [34], we have provided additional evidence that the degree of stemness followed the pattern: Stem-H > Stem-M > Stem-L among the subtypes ($P < 0.001$) (Fig. 1B). Survival analyses illustrated that Stem-H and Stem-L had the best and worst OS and DFS prognoses, respectively (Fig. 1C). Furthermore, we compared several cancer-associated features, such as epithelial-mesenchymal transition (EMT), metastasis, differentiation, invasion, and proliferation, among the three stemness subtypes. As anticipated, these features demonstrated the highest enrichment in Stem-H and the lowest enrichment in Stem-L ($P < 0.05$) (Fig. 1D and Supplementary Fig. S1A). Conversely, tumour purity likely followed the pattern: Stem-H < Stem-L ($P < 0.05$) (Fig. 1E). Furthermore, Stem-H contained a higher proportion of late-stage tumours than Stem-L ($P < 0.05$) (Fig. 1F).

The cell cycle is an indispensable process in cell biology, and any changes to this mechanism may result in pathological conditions, such as tumorigenesis [35]. We compared the mean expression of G1/S (DNA replication and division) and G2/M (DNA replication) marker genes between Stem-H and Stem-L. As anticipated, consistent in all five datasets, Stem-H exhibited greater average expression of G1/S and G2/M marker genes than Stem-L (Fig. 1G and Supplementary Figure S1B).

Pseudotime analysis revealed that most Stem-L tumours were in the onset or early stages of the trajectory, whereas most Stem-H tumours were in the terminal or later stages of the trajectory (Fig. 1H and Supplementary Fig. S1C). The results imply a connection between the stemness level and cancer progression.

To address the impact of tumour purity on the associations between glioma stemness subtypes and stemness and EMT signature scores, we developed logistic regression models that incorporated two predictors (stemness cluster and tumour purity) to predict stemness scores and EMT signature scores across the five datasets. This analysis showed that the stemness cluster positively predicted stemness and EMT scores (Supplementary Fig. S1D). Conversely, tumour purity negatively predicted stemness and EMT scores (Supplementary Fig. S1D). These results indicate that the significant linkages between the glioma stemness subtypes and stemness and EMT signatures are not contingent on tumour purity.

3.2. The stemness subtypes of glioma have significantly different genomic features

The phenomenon of genomic instability entails an increase in novel mutations within the genome, consequently propelling tumour progression and resistance toward therapy [36]. In the TCGA-glioma cohort, we observed a significantly higher TMB in Stem-H compared to Stem-L ($P < 0.001$) (Fig. 2A). Homologous Recombination (HR) is a DNA repair process that involves several mediators [37]. Homologous recombination deficiency (HRD) can cause tumorgenesis and genomic instability [38]. We found that HRD scores were significantly higher in Stem-H than in Stem-L in the TCGA-glioma dataset ($P < 0.05$) (Fig. 2B). Additionally, The G-scores of copy number amplifications and deletions were the highest in the Stem-H and the lowest in the Stem-L (Fisher's exact test, $P < 0.01$, Fig. 2C). ITH is a consequence of genomic instability and is linked to unfavorable outcomes in cancer [39]. Unsurprisingly, we found that Stem-H and Stem-L displayed the highest and lowest degree of ITH, respectively ($P < 0.01$) (Fig. 2D). Furthermore, we found that DNA repair pathways, such as mismatch repair and homologous recombination, had the highest and lowest enrichment levels in Stem-H and Stem-L, respectively ($P < 0.001$) (Fig. 2E). Moreover, many DNA damage response-related genes (*MSH2*, *MSH6*, *POLE*, and *POLD1*) showed the highest and lowest enrichment levels in Stem-H and Stem-L, respectively ($P < 0.001$) Fig. 2F).

O6-Methylguanine-DNA Methyltransferase (MGMT) promoter methylation is a strong prognostic factor in GBM therapy [40]. It is positively associated with the response to chemotherapy and overall survival [40]. As expected, the degree of MGMT promoter methylation was remarkably lower in Stem-H than in Stem-L in the TCGA glioma cohort (Chi-square test, $p < 0.0001$) (Fig. 2G). In contrast, Stem-L

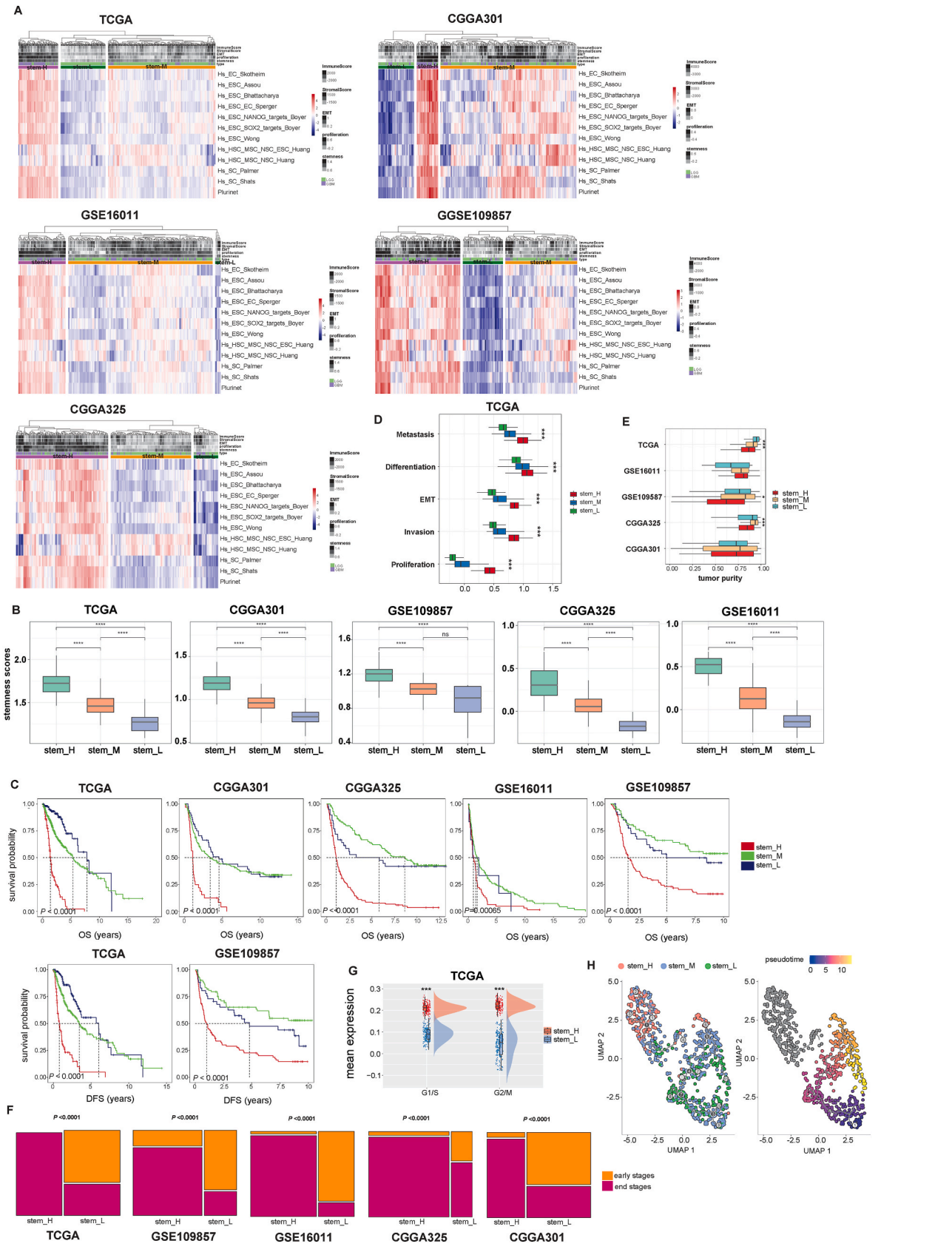

(caption on next page)

Fig. 1. Identification and characterization of stemness subtypes of glioma in bulk tumours. **A.** Hierarchical clustering identifying three stemness subtypes, Stem-H, Stem-M, and Stem-L, consistent in five different datasets, based on the enrichment scores of 12 stemness gene sets. **B.** Comparison of the enrichment scores of a stemness signature consisted of 109 genes among stemness subtypes of glioma (one-tailed Mann–Whitney *U* test). **C.** Kaplan–Meier curves show that Stem-H and Stem-L likely have the best and worst overall survival (OS) and/or disease-free survival (DFS) prognosis, respectively (log-rank test). **D.** Comparisons of the enrichment scores of five biological processes among stemness subtypes in TCGA glioma (ANOVA test). **E.** Comparisons of tumour purity across stemness subtypes within the five datasets (ANOVA test). **F.** Comparisons of the proportion of late-stage tumours between Stem-H and Stem-L within the five datasets (chi-square test). **G.** Comparison of the G1/S and G2/M cell cycle phases mean expression between Stem-H and Stem-L in the TCGA glioma (one-tailed Mann–Whitney *U* test). **H.** Pseudotime analysis showing the trajectory paths of the stemness subtypes in TCGA glioma. *P*-values are shown. $^{*}P < 0.05$, $^{**}P < 0.01$, $^{***}P < 0.001$, ^{ns} not significant.

contained a significantly higher proportion of MSI cancers than Stem-H ($P < 0.05$) (Fig. 2H and Supplementary Figure S2A). Overall, these data suggested a higher extent of genomic instability in Stem-H tumours compared with Stem-L tumours.

3.3. The stemness subtypes have significantly different immune microenvironments and responses to immunotherapy

Immune cytolytic activity, an indicator of cancer immunity, is calculated from the mRNA expression levels of *GZMA* and *PRF1* [41]. We found that Stem-H demonstrated noticeably higher cytolytic activity than Stem-L in the TCGA-glioma cohort (Fig. 3A). The human leukocyte antigen (HLA) is responsible for presenting tumour antigens to T cells, thereby accelerating the immune system's ability to recognize tumour cells [42]. The expression levels of most HLA genes showed the pattern: Stem-H > Stem-L (Fig. 3B). In addition, we evaluated the proportions of 22 immune cell subsets between the stemness subtypes of glioma using the CIBERSORT algorithm. We found that the Stem-H subtype had significantly higher proportions of neutrophils, mast cells activated, dendritic cells activated, macrophages, T cells regulatory, T cells CD4 memory resting, NK cells activated, cells follicular helper, and plasma cells than the Stem-L subtype (Fig. 3C). These results suggest that the stemness signature is positively associated with the anti-tumour immune response.

Furthermore, we predicted the response rates to immune checkpoint inhibitors (ICIs) in the stemness subtypes of glioma by the TIDE algorithm [30]. The TIDE scores are used to describe the prediction responses, where a higher score indicates a greater potential for tumour immune evasion and a lower likelihood of benefiting from ICIs treatments. Our analysis revealed that Stem-H had consistently higher TIDE scores across four datasets (TCGA-glioma cohort, GSE109857, CGGA301, and CGGA325) than Stem-M and Stem-L (Fig. 3D). This result is justified, since Stem-H has the highest TMB levels and immune infiltration.

3.4. The stemness subtypes have distinct mutation profiles

The emergence of cancers is ascribed to modifications in the DNA sequence of genomes, and genes that expedite tumour growth by mutation are acknowledged as driver genes [43]. The maftools function "oncodrive" [44] was employed for the identification of driver cancer genes from a provided MAF. Our discovery of top cancer driver genes was based on positional clustering, which revealed their enrichment at a few specific loci. We compared the mutation frequencies of the top detected 147 driver genes among the stemness subtypes in the TCGA-glioma cohort (Supplementary Table). Notably, Stem-H exhibited the highest mutation rate in numerous cancer driver genes, such as *PTEN*, *EGFR*, *TP53*, *PIK3CA*, *PDGFRA, TTN, IDH1, ATRX, MUC16,* and *NF1*. *PTEN* is one of the most frequently mutated tumour suppressors, especially in glioma [45]. Our analysis showed that *PTEN* had an extremely high mutation rate (84%) in Stem-H, consistent with previous reports that the high frequency of *PTEN* mutation was associated with poor prognosis in glioma patients (Fig. 4A–B) [45]. 50% of tumours, especially glioma with *EGFR* amplification mutants, are highly oncogenic [46]. Our results indicate that Stem-H harbored a high frequency (79%) of the *EGFR* amplification mutant, indicating a strong association between stemness and *EGFR* mutation in glioma (Fig. 4A–B). *TP53* is the most frequently mutated gene in cancer. As expected, Stem-H displayed the highest mutation rate of *TP53* among the stemness subtypes (Fig. 4A). We further analyzed the association between survival and the 10 most frequently mutated genes (*PTEN*, *EGFR*, *TP53*, *PIK3CA*, *PDGFRA*, *TTN*, *IDH1*, *ATRX*, *MUC16*, and *NF1*) in glioma. This analysis uncovered a significant correlation between the mutations of *PTEN*, *EGFR*, *PDGFRA*, *TTN*, and *NF1* and poor survival (Fig. 4B). Conversely, a better survival was associated with the mutations of *IDH1, TP53*, and *ATRX* (Fig. 4B).

3.5. The stemness subtypes have distinct protein expression profiles

Based on the TCGA-glioma protein expression data, we analyzed the expression levels of 166 proteins in the glioma stemness subtypes (Supplementary Table). We found 106 proteins were significantly differentiated between Stem-H and Stem-L, such as Cyclin B1, SMAD1, RBM15, RAD50, and ATM (FDR <0.05, Supplementary Table). Mutations in Cycline B1, SMAD1, RBM15, RAD50 have been found to play a significant oncogenic role and contribute to cancer progression [47–50]. The ATM protein played a pivotal role in the initiation of cell death [51]. We found that several proteins encoded genes function in different pathways, such as the PI3K-Akt signaling pathway, Neurotrophin signaling pathway, HIF-1 signaling pathway, FoxO signaling pathway, ErbB signaling pathway, EGFR tyrosine kinase inhibitor resistance, regulation of epithelial cell proliferation, regulation of apoptotic signaling pathway, positive regulation of DNA metabolic, and myeloid cell homeostasis (Fig. 5A). Furthermore, the stem-H cluster exhibits higher enrichment levels in mitotic cell cycle phase transition, regulation of TOR signaling, and regulation of apoptotic signaling pathway compared to the stem-L cluster (Fig. 5B). Collectively, the dysregulated pathways indicate a correlation between cancer stemness and cell survival, proliferation, and metabolic alterations. The activation of certain pathways can facilitate tumour inception and sustainment of cancer stem cell populations.

3.6. Identifying pathways and GO highly enriched in the stemness subtypes of glioma

We performed a weighted gene co-expression network analysis of the TCGA-glioma dataset by WGCNA. This analysis identified a set of 24 gene modules that significantly differentiated glioma by stemness subtypes. As expected, the gene modules associated with the cell cycle, angiogenesis, and cytoplasm were highly enriched in Stem-H ($r > 0.4$) (Fig. 6A). Moreover, vasculogenesis, immune response, lymphocyte activity, and metabolic process regulation were also enriched in Stem-H ($r > 0.15$) (Fig. 6A).

Furthermore, the application of pathway analysis through GSEA identifies multiple pathways that exhibited significant enrichment in the Stem-H subtype. These pathways primarily played a role in oncogenic and metabolic processes. As anticipated, our findings indicate a significant enrichment of telomere maintenance, DNA replication regulation, negative telomere maintenance regulation, mismatch repair, homologous recombination, epithelial to mesenchymal transition, DNA replication, DNA repair, and chromosome segregation in Stem-H compared to Stem-L in all five datasets (Fig. 6B–C, Supplementary Figs. S3A–C).

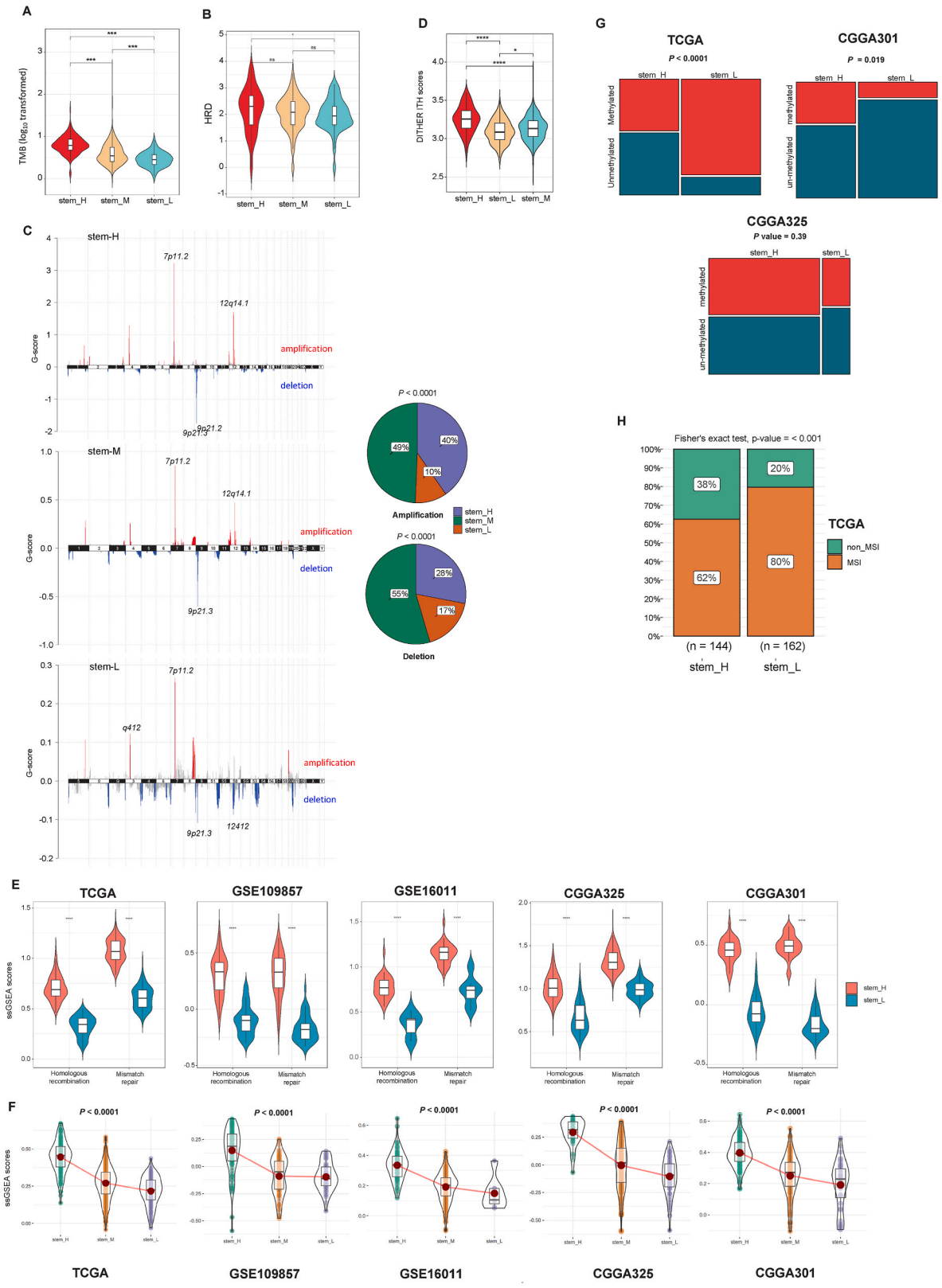

Fig. 2. Genomic features of the glioma subtypes. **A.** Tumour mutation burden among stemness subtypes in TCGA glioma (*t*-test). **B.** Homologous recombination deficiency (HRD) scores among stemness subtypes in TCGA glioma (*t*-test). **C.** G-scores among the stemness subtypes in TCGA glioma (chi-square test). **D.** ITH levels scores among the stemness subtypes in TCGA glioma (one-tailed Mann–Whitney *U* test). **E.** Comparisons of the enrichment scores of DNA damage repair pathways (mismatch repair and homologous recombination) among the stemness subtypes within the five datasets (one-tailed Mann–Whitney *U* test). **F.** The mean expression levels of DNA damage response genes among the stemness subtypes within the five datasets (Kruskal–Wallis test). **G.** The proportion of the MGMT promoter methylation between Stem-H and Stem-L in TCGA glioma, CGGA301, and CGGA325 (chi-square test). **H.** The proportion of MSI tumours among Stem-H and Stem-L in TCGA glioma (Fisher's exact test). *P*-values are shown. $^{*}P < 0.05$, $^{**}P < 0.01$, $^{***}P < 0.001$, ^{ns} not significant.

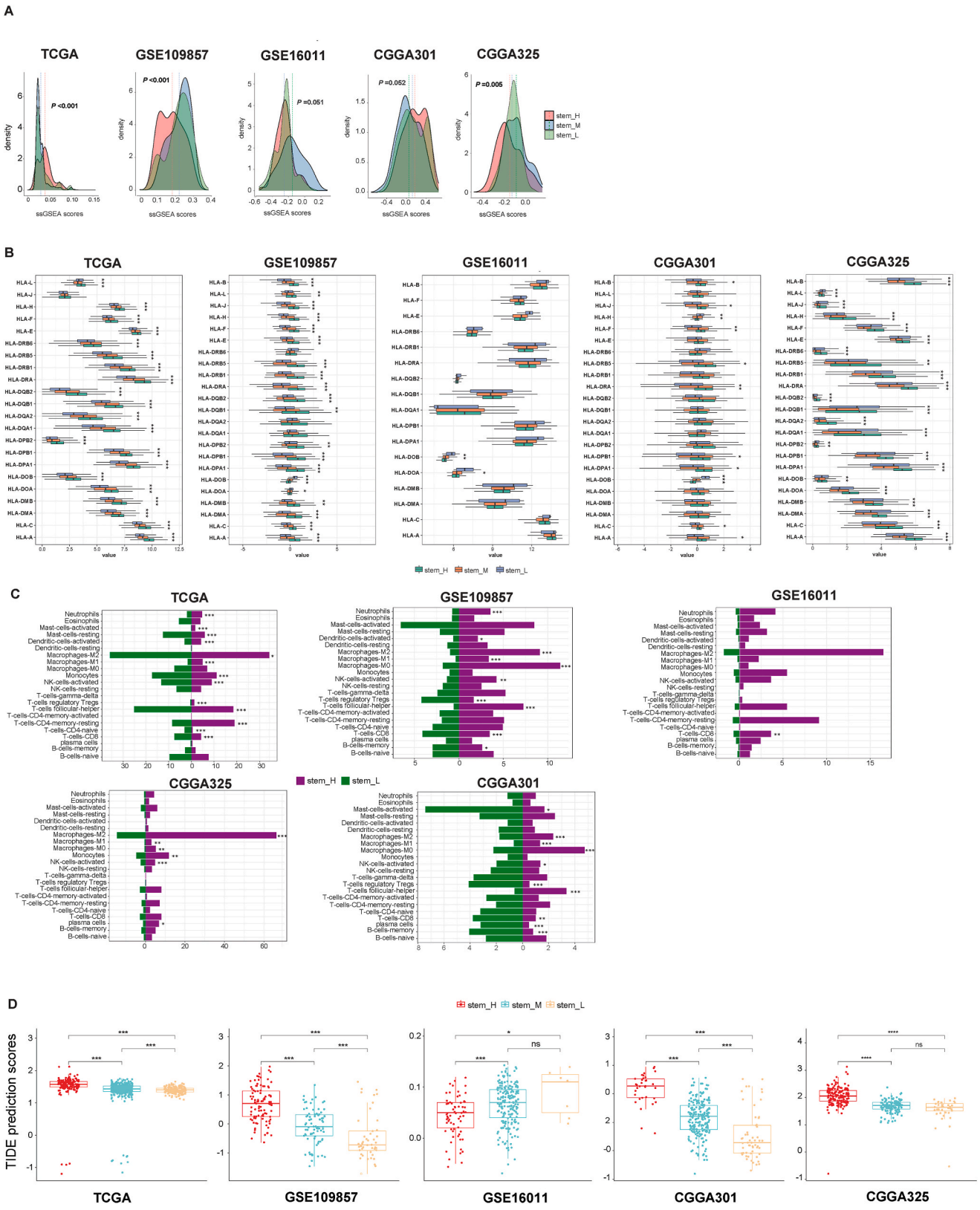

Fig. 3. The association between glioma stemness subtypes and the immune microenvironment and their response to immunotherapy. **A.** The cytolytic activity scores among the stemness subtypes within the five datasets. **B.** Comparisons of human leukocyte antigen (HLA) gene expression levels among the stemness subtypes within the five datasets (Kruskal–Wallis test). **C.** The proportion of the 22 immune cells between Stem-H and Stem-L within the five datasets using the CIBERSORT algorithm (one-tailed Mann–Whitney *U* test). **D.** The predicted response rates to immune checkpoint inhibitors among the stemness subtypes in the five datasets (*t*-test). *P*-values are shown. $^{*}P < 0.05$, $^{**}P < 0.01$, $^{***}P < 0.001$, ^{ns} not significant.

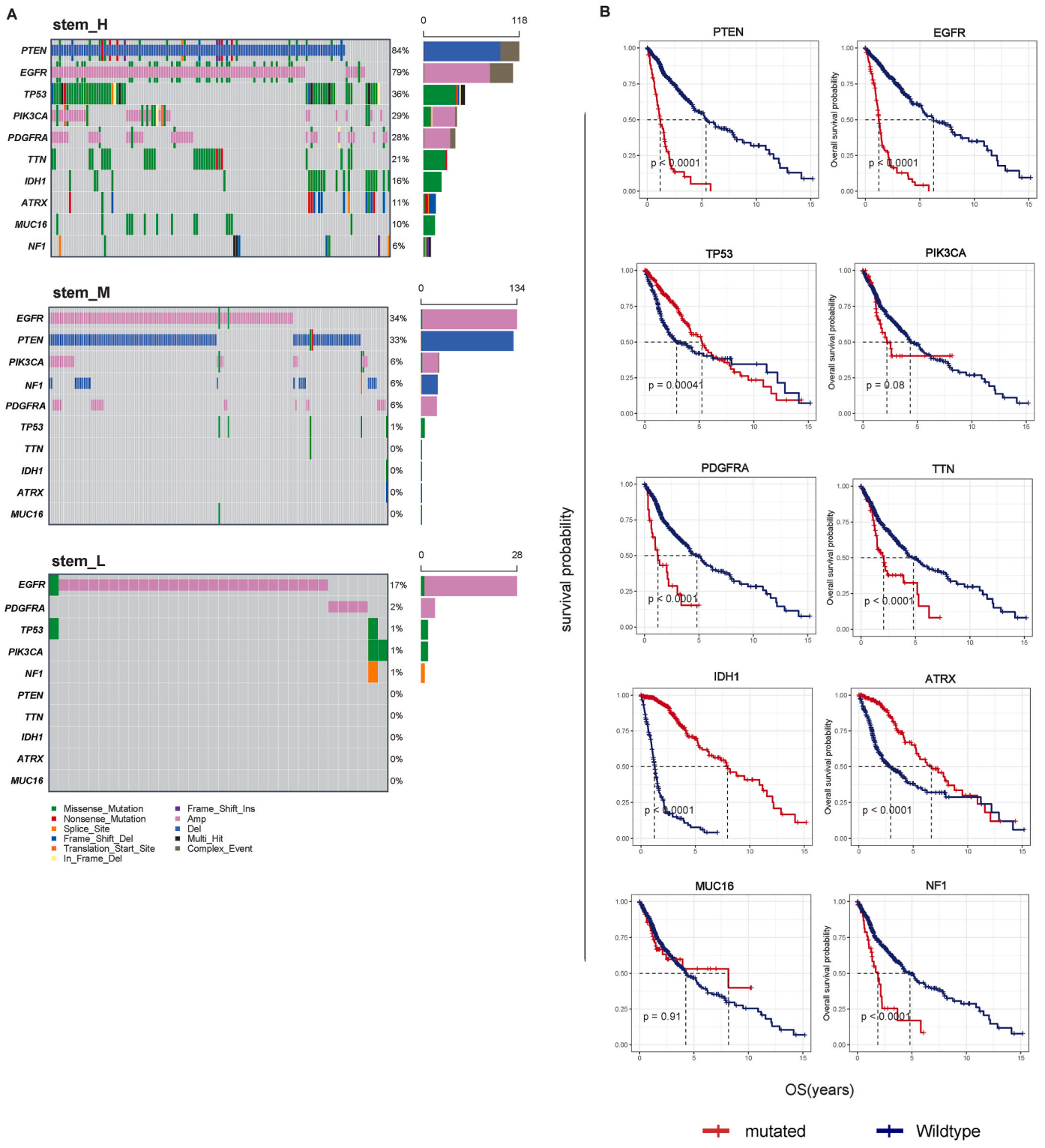

Fig. 4. Comparison of the mutation profiles between the glioma subtypes. **A.** Top 10 mutated genes showing significantly different mutation frequencies among the three glioma subtypes in the TCGA glioma dataset. **B.** Top 10 mutated genes whose mutation correlated with worse or better survival in the TCGA glioma dataset (log-rank test).

Telomere maintenance enables cancer cells to undergo indefinite cell division, resulting in uncontrolled cell proliferation and tumour growth [52]. Moreover, the occurrence of dysfunctional telomeres can lead to chromosomal instability, resulting in a diverse array of genetic mutations [52].

Additionally, the regulation of chromosome segregation involves multiple genes and proteins [53]. Chromosomal instability can occur when these genes undergo mutations or dysregulation, thus interrupting the normal process [53]. To provide an example, the impairment of the cell's ability to halt the cell cycle in response to chromosome segregation errors, as seen in mutations of tumour suppressor genes like TP53 (as indicated in stem-H), can result in the generation of genetic diversity

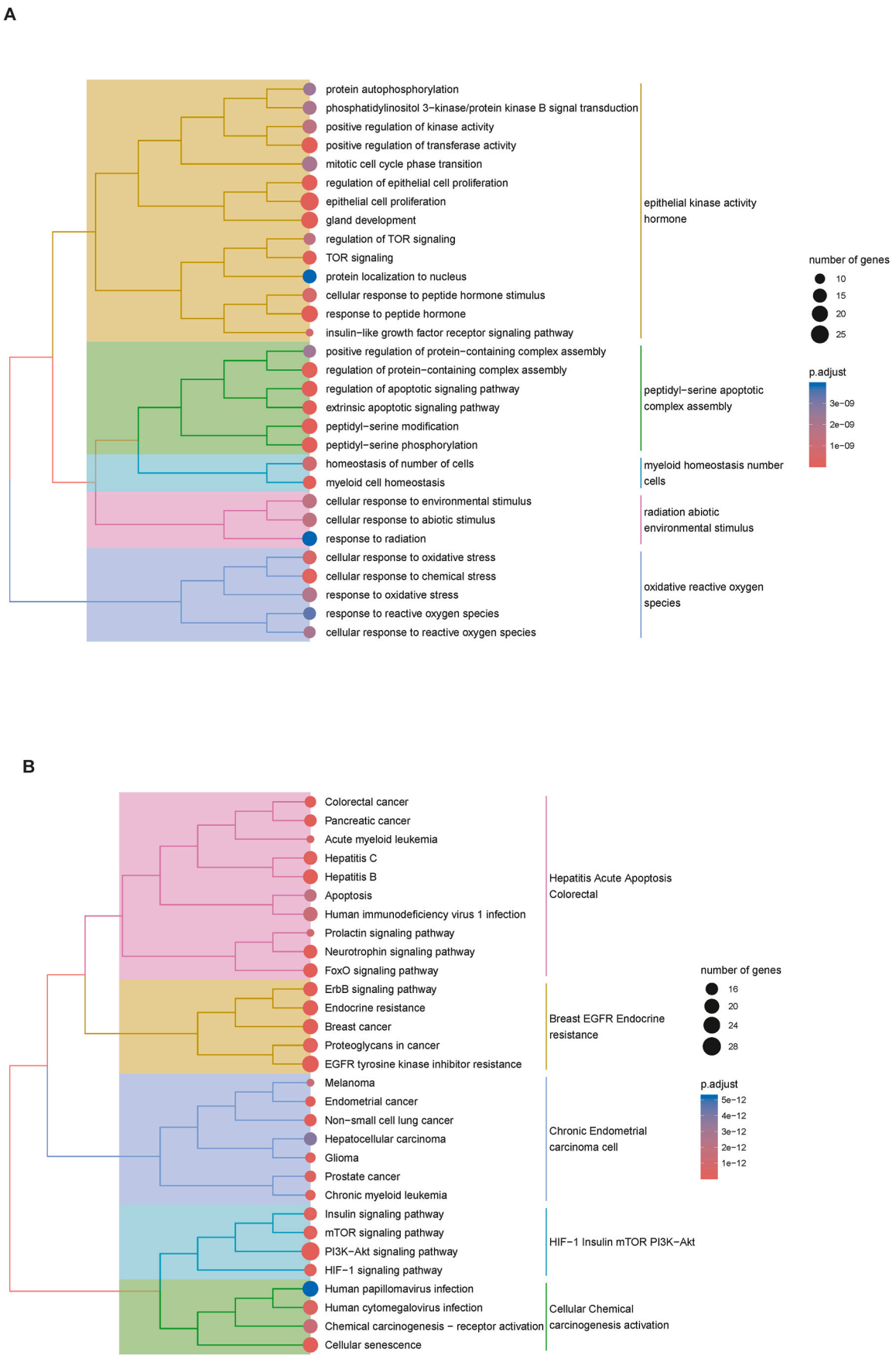

Fig. 5. The protein-encoding gene pathway enrichment analysis within the TCGA glioma stem-H cluster. **A.** The top enriched GO pathways and **B.** KEGG pathways, as determined by protein expression levels in Stem-H.

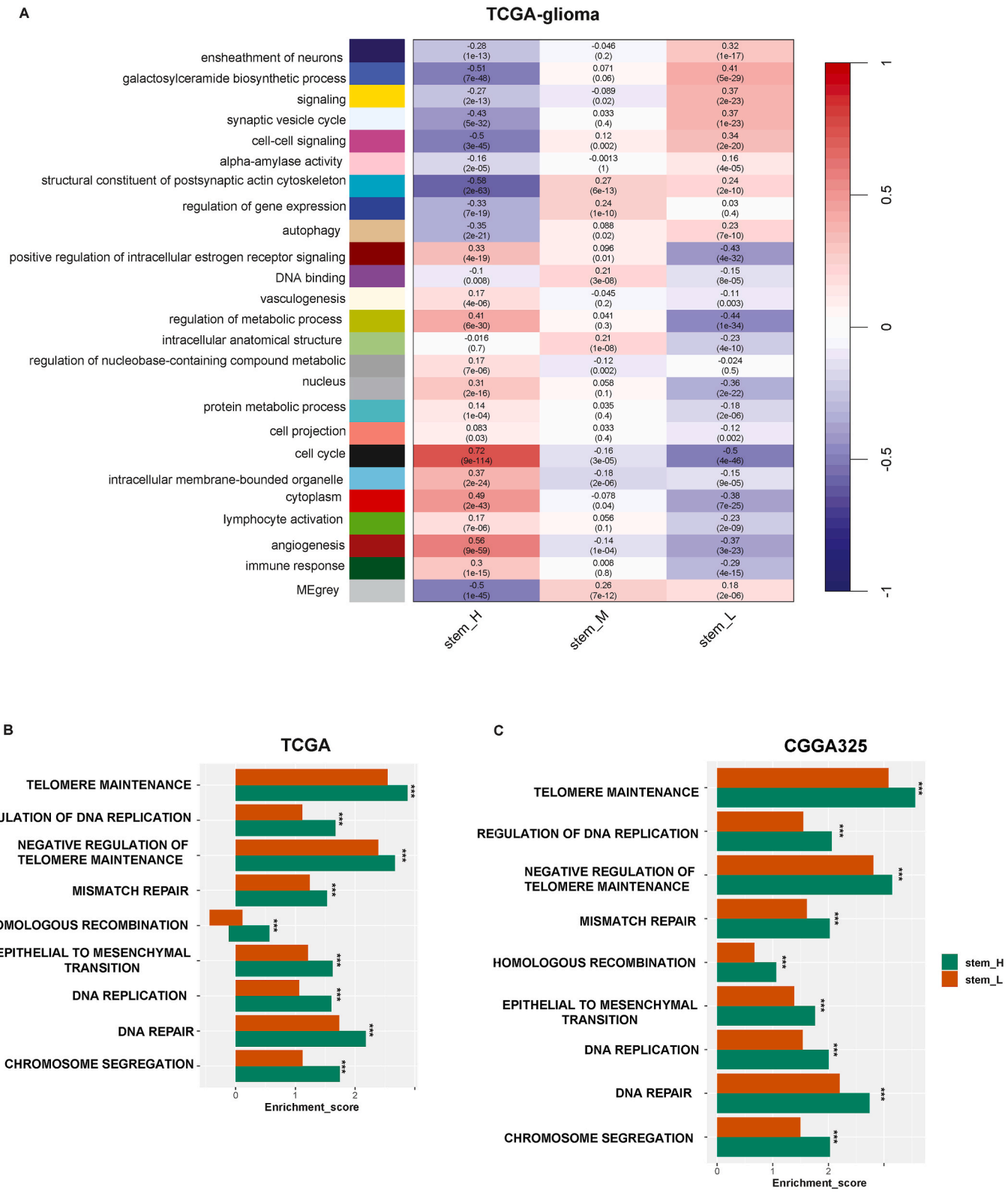

Fig. 6. Comparisons of pathway activity and gene ontology between the glioma stemness subtypes. **A.** 24 gene modules (gene ontology) that significantly differentiated gliomas by subtype identified by WGCNA. **B.** GO pathways highly enriched in the Stem-H and Stem-L of TCGA glioma and **C.** CGGA325 identified by GSEA. The correlation coefficients and *P*-values in parenthesis are shown.

within a tumour [53,54].

3.7. Identification of stemness subtypes of glioma single cells

To examine the replicability of the stemness-based subtyping approach at a single-cell level, we analyzed a glioma scRNA-seq dataset,

which comprised three distinct single-cell cohorts for glioma, namely GSE131928, GSE89567, and GSE57872. Based on the enrichment scores of the 12 stemness signatures, the cancer cells were evidently categorized into three subgroups, also termed Stem-H, Stem-M, and Stem-L, which displayed high, medium, and low enrichment scores of stemness signatures, respectively (Fig. 7A). The stemness levels and enrichment scores of proliferation, EMT, and invasion in two datasets, GSE131928 and GSE89567, demonstrated a Stem-H > Stem-L pattern, in accordance with the findings observed in bulk tumours ($P < 0.001$) (7B and Supplementary Fig. S4A). Among the two datasets (GSE131928 and GSE89567), Stem-H and Stem-L single cells exhibited the highest and lowest levels of enrichment levels of DNA damage response genes, respectively (Fig. 7C and Supplementary Fig. S4B). It indicated that Stem-H single cells had a higher degree of genomic instability than Stem-L single cells, consistent with the result shown in tumour bulks.

Pseudotime analysis showed that most Stem-H single cells were in the onset or early stages of the trajectory, whereas most Stem-L single cells were in the terminal or later stages of the trajectory (Fig. 7D and Supplementary Figs. S4C–D). The gene ontology analysis indicated that cancer cells characterized by high stemness were enriched in biological processes of cell cycle, DNA replication, fibroblast proliferation, mismatch repair, and cellular response to DNA damage, as compared to their low stemness counterparts (Fig. 7E and Supplementary Fig. S4E). Furthermore, we compared the cell cycle activity based on the mean expression of G1/S and G2/M between Stem-H and Stem-L. Consistent with the results from tumour bulks, Stem-H exhibited greater cell cycle activity than Stem-L (Fig. 7F and Supplementary Fig. S5A). In the GSE131928 dataset, we discovered that the MGMT promoter methylation level in Stem-H was lower than non-methylated group, while the *TP53* mutation rate was higher in Stem-H than Stem-L. Also, the EGFR mutation rate was higher in Stem-H than in Stem-L (Fig. 8A). Again, these findings are consistent with those in tumour bulks.

We clustered all single cells in three datasets by t-SNE [55]. The majority of Stem-H cells were distanced from Stem-L cells (Fig. 8B and Supplementary Fig. S5B). Moreover, the Stem-H cluster exhibited a closer proximity to the T cells and B cells cluster compared to the Stem-L cluster, whereas the Stem-L cluster displayed a closer proximity to the monocytes (Fig. 8B and Supplementary Fig. S5B).

4. Discussion

Glioma is a tremendous challenge that oncologists face due to its aggressive nature and limited treatment options [56]. In terms of the degrees of malignancy, glioma can be divided into Glioblastoma (GBM) and Lower-Grade Glioma (LGG). GBM is a highly malignant type of glioma, known as its resistance to conventional treatments and elevated relapse rates [57]. Conversely, LGG denotes a particular type of glioma that is distinguished by a slower rate of growth but still poses significant clinical challenges [58]. The concept of stemness holds paramount significance in the realm of neuro-oncology. The comprehension of the biology of brain tumours and the challenges in developing effective treatments is reliant on the understanding of glioma stem cells (GSCs) [59]. GSCs, similar to healthy neural stem cells, have the ability to self-renew and generate differentiated offspring [60]. Mounting evidence suggests that this exceptional characteristic significantly impacts the development, progression, recurrence, and chemo- and radio-resistance of gliomas [61,62]. Therefore, it is of utmost significance to examine the function of GSCs in facilitating the growth of glioma and in resistance towards therapy.

Prior investigations have exhaustively examined the molecular subtypes and predicated stemness characteristic of glioma, using bulk RNA-seq data [10,11]. Nonetheless, these prior discoveries may not comprehensively tackle the crucial facet of ITH, which is prevalent in glioma [63,64]. The analysis of RNA-seq in bulk may potentially mask the characteristics of crucial subpopulations of cells, particularly GSCs. In comparison, the analysis of scRNA-seq can effectively identify and classify rare cells, distinguish cancer cells from stromal cells and different immune cells, and provide a comprehensive perspective on the interrelationships among these constituents [65]. The primary objective of this study was to introduce a new clustering method for glioma classification, which relies on stemness and utilizes both bulk and single-cell RNA-seq data. The stemness-based subtyping method would assist in our comprehension of the complexity and heterogeneity of glioma and provide potential clinical implications for the management of this disease. Our results from scRNA-seq data analysis revealed that the gliomas with low stemness had a higher level of heterogeneity in the distribution of cancer cells. It is reasonable as tumours with low stemness originate from those with high stemness to result in their increased diversity. Indeed, the single-cell pseudotime analysis demonstrates the evolutional path from Stem-H to Stem-L tumours.

Elevated genomic instability is a common characteristic of Stem-H tumours, as indicated, for instance, by higher TMB, HRD scores, and DNA repair activity in bulk analysis. The presence of genomic instability in Stem-H gliomas indicates a heightened probability of therapy resistance and a more aggressive disease progression. Furthermore, the elevated mutation rates of driver genes, specifically PTEN, EGFR, and TP53, were observed in the Stem-H subtype in both bulk and single-cell analyses. Moreover, discrepancies in methylation levels at the MGMT promoter among stemness subtypes demonstrate distinct epigenetic regulatory pathways among various glioma subtypes. The methylation patterns can significantly impact on gene expression and DNA repair processes, consequently influencing genomic stability and therapeutic responses. The lower methylation of MGMT promoter found in Stem-H gliomas may affect their response to certain therapeutic interventions [66].

The concurrence of the findings in both bulk tumour and single-cell analyses underscores the robustness and credibility of the observed patterns in glioma stemness subtypes. As an illustration, it was determined that the Stem-H subtype exhibits more aggressive malignant characteristics in comparison to the Stem-L subtype. There was evidence of heightened proliferative potential indicated by increased expression of genes associated with cell cycle progression (G1/S and G2/M). Stem-H patients demonstrated reduced survival rates, a trend that was also corroborated by the high prevalence of mutations in key glioma-driver genes such as PTEN, EGFR, and TP53. Moreover, Stem-H tumours were consistently linked with the disturbance of critical pathways that govern cellular survival, proliferation, and metabolic modifications, such as PI3K-Akt, HIF-1, and EGFR signaling, in both bulk and single-cell analyses. These results emphasize the significance of these pathways in glioma stemness.

Our results differ from the previous related research, which classified glioma into two groups [10], as we were able to categorize them into three subtypes: Stem-H, Stem-M, and Stem-L. In contrast to Stem-H and Stem-L, Stem-M demonstrated distinct genomic and mutational traits. Moreover, the existence of three subclasses intensifies the diversity between the groups enriched with high and low stemness. This enabled us to obtain more precise comparisons among various subclasses. Moreover, the previous study's classification was based on stemness index and limited to RNA-seq's bulk data. Our analysis explored the glioma stemness based on both bulk and single-cell data, thereby providing a broader perspective on the distinguishing characteristics of each subclass.

Although our study offers valuable insights into glioma classification based on stemness using both bulk and single-cell RNA-seq data, it is crucial to acknowledge specific limitations that could affect the interpretation and generalization of our findings. Initially, the incorporation of data from various sources and platforms can introduce heterogeneity, which may impact the reliability of our classifications. The potential impact of variations in data collection methods and technologies on result consistency across datasets should be considered. Additionally, the potential impact on the generalizability of the identified subtypes should be considered in light of the number and diversity of samples

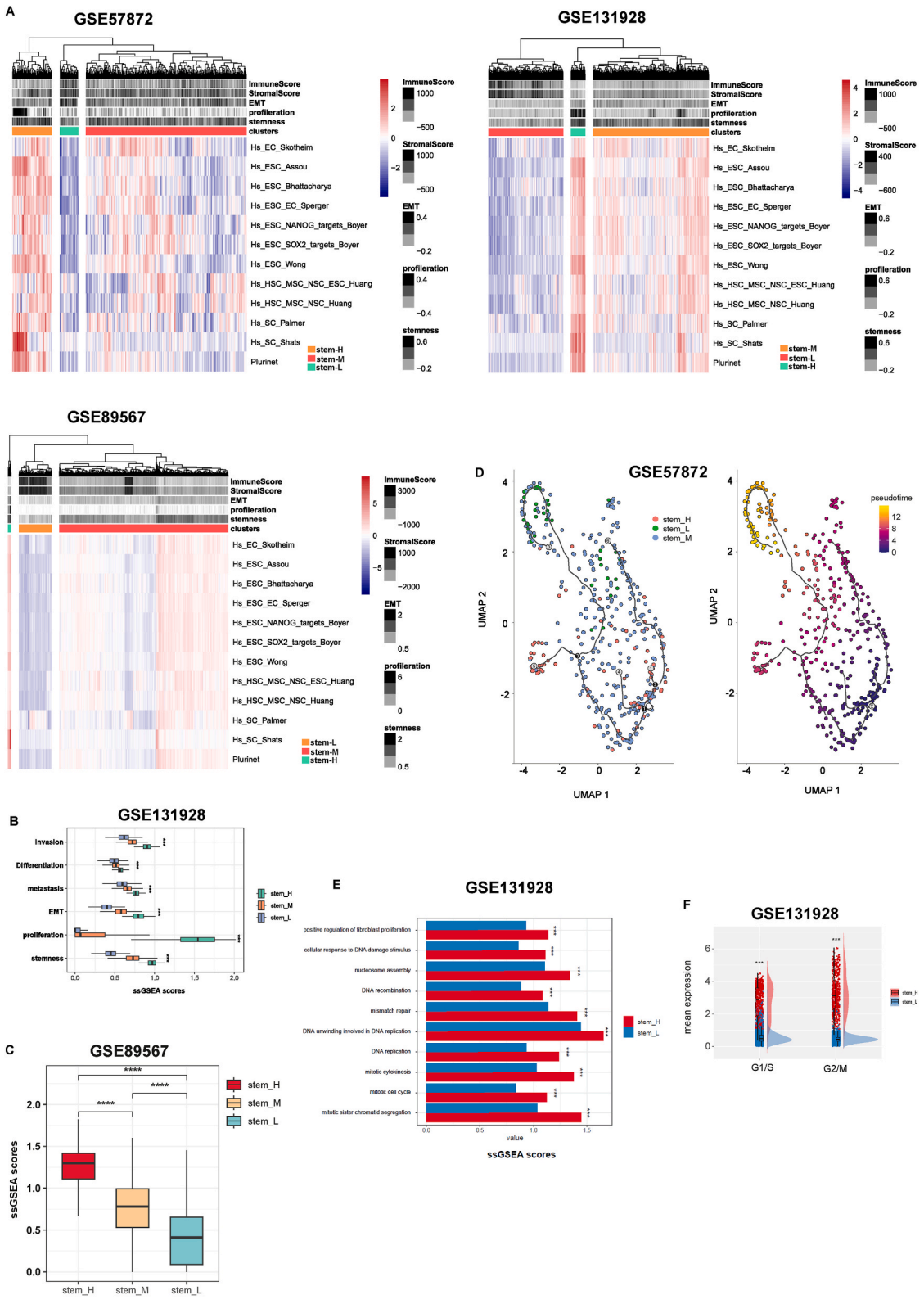

Fig. 7. Identification of stemness subtypes of glioma single cells. **A.** Hierarchical clustering identifying three stemness subtypes, Stem-H, Stem-M, and Stem-L, consistent in three different datasets, based on the enrichment scores of 12 stemness gene sets. **B.** Comparison of the enrichment scores of the stemness signature and five biological processes in the GSE131928 single cells (Kruskal–Wallis test). **C.** Comparison of the mean expression of DNA damage response genes among stemness subtypes in the GSE89567 single cells (one-tailed Mann–Whitney *U* test). **D.** Pseudotime analysis showing the trajectory paths of the stemness subtypes in the GSE57872 single cells. **E.** Gene set enrichment analysis identifying the biological process terms enriched in Stem-H and Stem-L in the GSE131928 single cells (*t*-test). **F.** Comparison of the G1/S and G2/M cell cycle phases mean expression between Stem-H and Stem-L in the GSE131928 single cells (one-tailed Mann–Whitney *U* test). *P*-values are shown. $^{*}P < 0.05$, $^{**}P < 0.01$, $^{***}P < 0.001$, ^{ns} not significant.

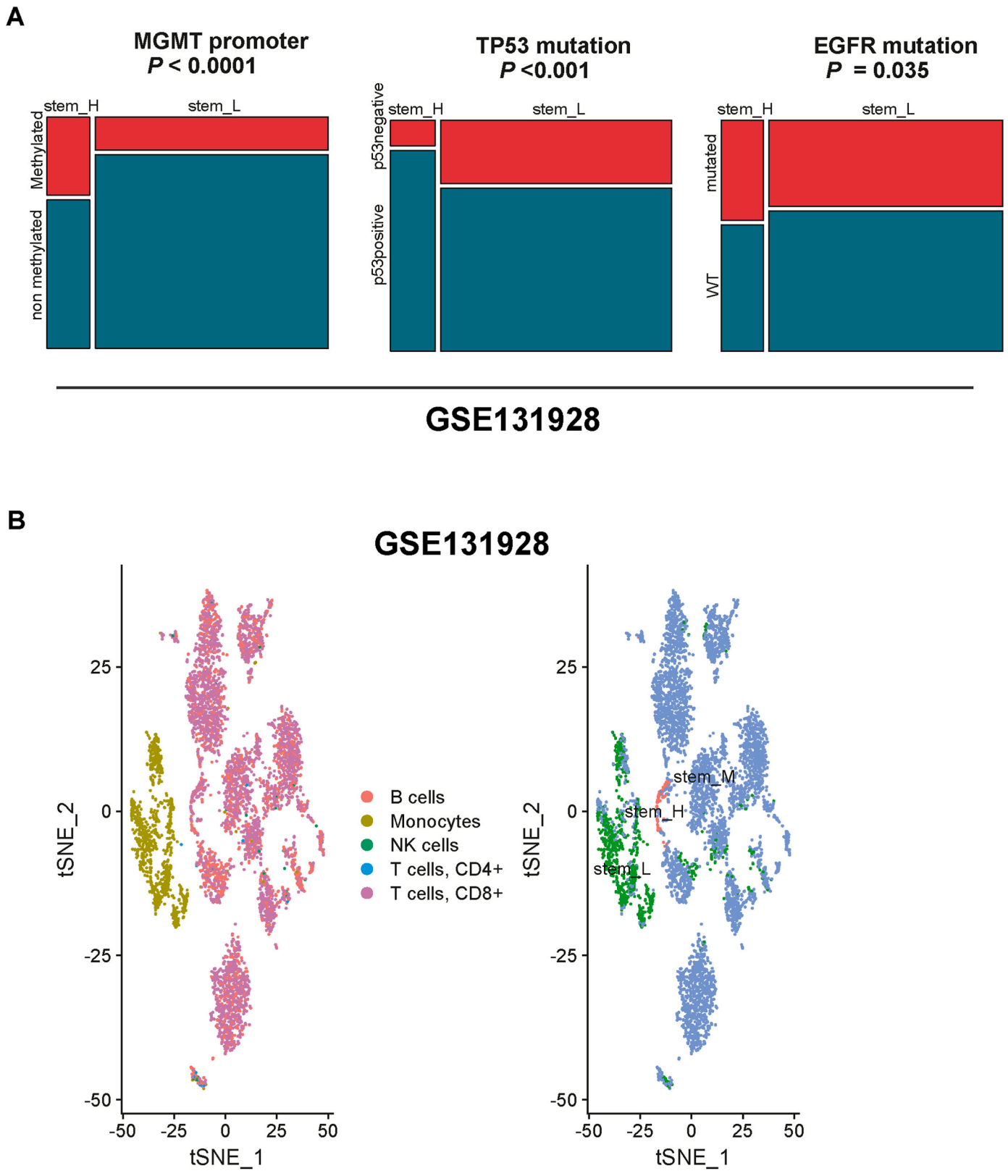

Fig. 8. Genomic features and the immune response among glioma single-cell subtypes. **A.** The proportion of the MGMT promoter methylation, TP53 mutation and EGFR mutation among Stem-H and Stem-L in the GSE131928 single cells (chi-square test). **B.** Clustering of the GSE131928 single cells by t-SNE. *P*-values are shown.

analyzed in our study. Implementing a larger and more diverse sample size would have a positive impact on the reliability of subtype characterization and the representation of the glioma population. In addition, our study reveals the molecular and genomic features correlated with different stemness subtypes. Nonetheless, further experimental verification is necessary to ascertain the biological implications of these findings. Finally, it should be noted that although our findings have significant clinical implications, there may be difficulties in translating

molecular subtypes into successful therapeutic approaches. The clinical utility of these subtypes necessitates further validation through larger patient cohorts and clinical trials.

In conclusion, this study has classified gliomas into three subtypes based on stemness and distinguished them by their molecular profiles. Gliomas of the Stem-H type display unfavorable outcomes, increased DNA repair activity, and possible resistance to immunotherapy. On the other hand, Stem-L gliomas exhibit a better prognosis and improved immune responses within the tumour microenvironment, yielding crucial clinical management insights.

Funding

This research did not receive any specific grant from funding agencies in the public, commercial, or not-for-profit sectors.

CRediT authorship contribution statement

Zeinab Abdelrahman: Writing – review & editing, Writing – original draft, Visualization, Validation, Software, Methodology, Investigation, Formal analysis, Data curation, Conceptualization. **Alaa Abdelatty:** Writing – original draft, Visualization, Methodology, Formal analysis. **Jiangti Luo:** Formal analysis. **Amy Jayne McKnight:** Writing – review & editing, Supervision. **Xiaosheng Wang:** Writing – review & editing, Supervision, Methodology, Formal analysis.

Declaration of competing interest

All authors declare that there is no conflict of interest.

Appendix A. Supplementary data

Supplementary data to this article can be found online at https://doi.org/10.1016/j.compbiomed.2024.108304.

References

[1] M. Weller, et al., Glioma, Nat. Rev. Dis. Prim. 1 (1) (2015) 15017.
[2] E. Parmigiani, et al., Old Stars and new Players in the brain tumor microenvironment, Front. Cell. Neurosci. 15 (2021) 709917.
[3] M. Weller, et al., Molecular Neuro-Oncology in Clinical Practice: a New Horizon, vol. 14, 2013, pp. e370–e379, 9.
[4] J.A. Joyce, D.T. Fearon, T cell exclusion, immune privilege, and the tumor microenvironment, Science 348 (6230) (2015) 74–80.
[5] P. Chen, et al., Cancer stemness Meets immunity: from mechanism to therapy, Cell Rep. 34 (1) (2021) 108597.
[6] A. Gieryng, et al., Immune microenvironment of gliomas, Lab. Invest. 97 (5) (2017) 498–518.
[7] J. Wu, J.C.I.J.C. Belmonte, Stem Cells: a Renaissance in Human Biology Research, vol. 165, 2016, pp. 1572–1585, 7.
[8] H.O. Kaseb, et al., Identification, Expansion and Characterization of Cancer Cells with Stem Cell Properties from Head and Neck Squamous Cell Carcinomas, vol. 348, 2016, pp. 75–86, 1.
[9] A.L.V. Alves, et al., Role of glioblastoma stem cells in cancer therapeutic resistance: a perspective on antineoplastic agents from natural sources and chemical derivatives, Stem Cell Res. Ther. 12 (1) (2021) 206.
[10] Z. Wang, et al., Machine learning revealed stemness features and a novel stemness-based classification with appealing implications in discriminating the prognosis, immunotherapy and temozolomide responses of 906 glioblastoma patients, Briefings Bioinf. 22 (5) (2021) bbab032.
[11] M. Zhang, et al., Prognostic value of a stemness index-associated signature in primary lower-grade glioma, Front. Genet. 11 (2020) 441.
[12] L.A. Gravendeel, et al., Intrinsic gene expression profiles of gliomas are a better predictor of survival than histology, Cancer Res. 69 (23) (2009) 9065–9072.
[13] B. Zhang, et al., Identification of prognostic Biomarkers for multiple solid tumors using a human villi development model, Front. Cell Dev. Biol. 8 (2020) 492.
[14] C. Neftel, et al., An integrative model of cellular states, plasticity, and genetics for glioblastoma, Cell 178 (4) (2019) 835–849.e21.
[15] A.S. Venteicher, et al., Decoupling genetics, lineages, and microenvironment in IDH-mutant gliomas by single-cell RNA-seq, Science 355 (6332) (2017).
[16] A.P. Patel, et al., Single-cell RNA-seq highlights intratumoral heterogeneity in primary glioblastoma, Science 344 (6190) (2014) 1396–1401.
[17] J.P. Pinto, et al., StemChecker: a web-based tool to discover and explore stemness signatures in gene sets, Nucleic Acids Res. 43 (W1) (2015) W72–W77.
[18] S. Hänzelmann, R. Castelo, J. Guinney, GSVA: gene set variation analysis for microarray and RNA-Seq data, BMC Bioinf. 14 (1) (2013) 7.
[19] R. Kolde, M.R. Kolde, Package 'pheatmap', R package 1 (7) (2015) 790.
[20] J.T. Rich, et al., A practical guide to understanding Kaplan-Meier curves, Otolaryngol. Head Neck Surg. 143 (3) (2010) 331–336.
[21] T.M. Therneau, T. Lumley, Package 'survival', R Top Doc. 128 (10) (2015) 28–33.
[22] G. Yu, et al., clusterProfiler: an R package for comparing biological themes among gene clusters, OMICS 16 (5) (2012) 284–287.
[23] P. Langfelder, S. Horvath, WGCNA: an R package for weighted correlation network analysis, BMC Bioinf. 9 (1) (2008) 559.
[24] C.H. Mermel, et al., GISTIC2.0 facilitates sensitive and confident localization of the targets of focal somatic copy-number alteration in human cancers, Genome Biol. 12 (4) (2011) R41.
[25] L. Li, C. Chen, X.J.B.i.B. Wang, DITHER: an Algorithm for Defining Intratumor Heterogeneity Based on Entropy, vol. 22, 2021, p. bbab202, 6.
[26] K. Yoshihara, et al., Inferring tumour purity and stromal and immune cell admixture from expression data, Nat. Commun. 4 (1) (2013) 2612.
[27] B. Chen, et al., Profiling tumor infiltrating immune cells with CIBERSORT, Cancer Syst. Biol.: Methods Protocols (2018) 243–259.
[28] B. Chen, et al., Profiling tumor infiltrating immune cells with CIBERSORT, Methods Mol. Biol. 1711 (2018) 243–259.
[29] X. Qiu, et al., Reversed graph embedding resolves complex single-cell trajectories, Nat. Methods 14 (10) (2017) 979–982.
[30] P. Jiang, et al., Signatures of T cell dysfunction and exclusion predict cancer immunotherapy response, Nat. Med. 24 (10) (2018) 1550–1558.
[31] D. Aran, et al., Reference-based analysis of lung single-cell sequencing reveals a transitional profibrotic macrophage, Nat. Immunol. 20 (2) (2019) 163–172.
[32] L. Van der Maaten, G.J.J.o.m.l.r. Hinton, Visualizing Data Using T-SNE, vol. 9, 2008, 11.
[33] Y. Benjamini, Y. Hochberg, Controlling the false discovery rate: a practical and powerful approach to multiple testing, J. Roy. Stat. Soc. B 57 (1) (1995) 289–300.
[34] A. Miranda, et al., Cancer stemness, intratumoral heterogeneity, and immune response across cancers, Proc. Natl. Acad. Sci. U. S. A. 116 (18) (2019) 9020–9029.
[35] K. Gousias, T. Theocharous, M. Simon, Mechanisms of cell cycle arrest and apoptosis in glioblastoma, Biomedicines 10 (3) (2022).
[36] K. Kang, et al., Genomic instability in lower-grade glioma: prediction of prognosis based on lncRNA and immune infiltration, Mol. Ther. Oncolyt. 22 (2021) 431–443.
[37] M. Toh, J.J.T.O. Ngeow, Homologous Recombination Deficiency: Cancer Predispositions and Treatment Implications, vol. 26, 2021, pp. e1526–e1537, 9.
[38] H. Wen, et al., Homologous recombination deficiency in diverse cancer types and its correlation with platinum chemotherapy efficiency in ovarian cancer, BMC Cancer 22 (1) (2022) 550.
[39] Y.C.S. Ramón, et al., Clinical implications of intratumor heterogeneity: challenges and opportunities, J. Mol. Med. (Berl.) 98 (2) (2020) 161–177.
[40] J. Feldheim, et al., Changes of O(6)-methylguanine DNA Methyltransferase (MGMT) promoter methylation in glioblastoma relapse-A meta-analysis type literature review, Cancers 11 (12) (2019).
[41] H. Wakiyama, et al., Cytolytic activity (CYT) score is a prognostic biomarker reflecting host immune status in hepatocellular carcinoma (HCC), Anticancer Res. 38 (12) (2018) 6631–6638.
[42] C. Wang, et al., Human Leukocyte Antigen (HLA) and Cancer Immunotherapy: HLA-dependent and -independent Adoptive Immunotherapies, vol. 2020, 2020, p. 5.
[43] S. Morjaria, S. Morjaria, Driver mutations in oncogenesis, Int. J. Mol. Immuno Oncol. 6 (2) (2021) 100–102.
[44] D. Tamborero, A. Gonzalez-Perez, N. Lopez-Bigas, OncodriveCLUST: exploiting the positional clustering of somatic mutations to identify cancer genes, Bioinformatics 29 (18) (2013) 2238–2244.
[45] J.-M. Yang, et al., Characterization of PTEN mutations in brain cancer reveals that pten mono-ubiquitination promotes protein stability and nuclear localization, Oncogene 36 (26) (2017) 3673–3685.
[46] K.J. Hatanpaa, et al., Epidermal growth factor receptor in glioma: signal transduction, neuropathology, imaging, and radioresistance, Neoplasia 12 (9) (2010) 675–684.
[47] Y. Li, et al., Rad50 promotes ovarian cancer progression through NF-κB activation, J. Cell Mol. Med. 25 (23) (2021) 10961–10972.
[48] Z. Zhao, et al., N6-Methyladenosine methylation regulator RBM15 is a potential prognostic biomarker and promotes cell proliferation in pancreatic adenocarcinoma, Front. Mol. Biosci. 9 (2022) 842833.
[49] Q. Wang, et al., SMAD Proteins in TGF-β Signalling Pathway in Cancer: Regulatory Mechanisms and Clinical Applications, vol. 13, 2023, p. 2769, 17.
[50] C. Ye, et al., Prognostic role of cyclin B1 in solid tumors: a meta-analysis, Oncotarget 8 (2) (2017) 2224–2232.
[51] T. Aki, K. Uemura, Cell death and survival pathways involving ATM protein kinase, Genes 12 (10) (2021).
[52] Jerry W. Shay, Woodring E. Wright, Telomeres and telomerase: three decades of progress, Nat. Rev. Genet. 20 (5) (2019) 299–309.
[53] N.J. Ganem, S.A. Godinho, D.J.N. Pellman, A Mechanism Linking Extra Centrosomes to Chromosomal Instability, vol. 460, 2009, pp. 278–282, 7252.
[54] A.J. Levine, M.J.N.r.c. Oren, The First 30 Years of P53: Growing Ever More Complex, vol. 9, 2009, pp. 749–758, 10.
[55] S.L. Carter, et al., Absolute quantification of somatic DNA alterations in human cancer, Nat. Biotechnol. 30 (5) (2012) 413–421.
[56] E.A. Maher, et al., Malignant glioma: genetics and biology of a grave matter, Genes Dev. 15 (11) (2001) 1311–1333.

[57] D.N. Louis, et al., The 2007 WHO classification of tumours of the central nervous system, Acta Neuropathol. 114 (2007) 97–109.
[58] R. Soffietti, et al., Guidelines on management of low-grade gliomas: report of an EFNS–EANO* Task Force, Eur. J. Neurol. 17 (9) (2010) 1124–1133.
[59] D.L. Schonberg, et al., Brain tumor stem cells: molecular characteristics and their impact on therapy, Mol. Aspect. Med. 39 (2014) 82–101.
[60] E.R. Matarredona, A.M. Pastor, Neural stem cells of the subventricular zone as the origin of human glioblastoma stem cells. Therapeutic implications, Front. Oncol. 9 (2019) 779.
[61] T.S. van Solinge, et al., Advances in local therapy for glioblastoma - taking the fight to the tumour, Nat. Rev. Neurol. 18 (4) (2022) 221–236.
[62] V. Mattei, et al., The importance of tumor stem cells in glioblastoma resistance to therapy, Int. J. Mol. Sci. 22 (8) (2021) 3863.
[63] M.-d.-M. Inda, R. Bonavia, J. Seoane, Glioblastoma multiforme: a look inside its heterogeneous nature, Cancers 6 (1) (2014) 226–239.
[64] K. Anjum, et al., Current status and future therapeutic perspectives of glioblastoma multiforme (GBM) therapy: a review, Biomed. Pharmacother. 92 (2017) 681–689.
[65] G. Chen, B. Ning, T. Shi, Single-cell RNA-seq technologies and related computational data analysis, Front. Genet. 10 (2019) 317.
[66] B. Kaina, M. Christmann, DNA repair in personalized brain cancer therapy with temozolomide and nitrosoureas, DNA Repair 78 (2019) 128–141.